Available online at www.sciencedirect.com
SCIENCE DIRECT®
Journal of Magnetic Resonance 162 (2003) 217–227
JMR Journal of Magnetic Resonance
www.elsevier.com/locate/jmr

Recoupled long-range C–H dipolar dephasing in solid-state NMR, and its use for spectral selection of fused aromatic rings

J.-D. Mao and K. Schmidt-Rohr*

Department of Chemistry, Gilman Hall, Iowa State University, Ames, IA 50010, USA

Received 23 September 2002; revised 13 January 2003

Abstract

This work introduces a simple new solid-state ^{13}C NMR method for distinguishing various types of aromatic residues, e.g. those of lignin from fused rings of charcoal. It is based on long-range dipolar dephasing, which is achieved by recoupling of long-range C–H dipolar interactions, using two ^{1}H 180° pulses per rotation period. This speeds up dephasing of unprotonated carbon signals approximately threefold compared to standard dipolar dephasing without recoupling and thus provides much more efficient differential dephasing. It also reduces the effects of spinning-speed dependent effective proton–proton dipolar couplings on the heteronuclear dephasing. Signals of unprotonated carbons with two or more protons at a two-bond distance dephase to <3% within less than 0.9 ms, significantly faster than those of aromatic sites separated from the nearest proton by three or more bonds. Differential dephasing among different unprotonated carbons is demonstrated in a substituted anthraquinone and 3-methoxy benzamide. The data yield a calibration curve for converting the dephasing rates into estimated distances from the carbon to the nearest protons. This can be used for peak assignment in heavily substituted or fused aromatic molecules. Compared to lignin, slow dephasing is observed for the aromatic carbons in wood charcoal, and even slower for inorganic carbonate. Direct ^{13}C polarization is used on these structurally complex samples to prevent loss of the signals of interest, which by design originate from carbons that are distant from protons and therefore crosspolarize poorly. In natural organic matter such as humic acids, this combination of recoupled dipolar dephasing and direct polarization at 7-kHz MAS enables selective observation of signals from fused rings that are characteristic of charcoal.

1. Introduction

A large fraction of the organic matter in the natural environment contains significant aromatic components [1]. In spite of their large contribution to the carbon pool in nature, these aromatic structures have remained quite poorly characterized. When multiply oxygen-substituted or fused aromatic rings are present, there are large numbers of different carbon sites with often overlapping NMR resonance lines [2–11]. This has made it difficult to characterize or even distinguish different types of aromatic compounds in natural organic matter. The large fraction of unprotonated aromatic carbons in such systems is not amenable to detailed solution NMR analysis, which always involves a proton NMR dimension [12].

A particularly stable form of aromatic carbon in the environment that has recently attracted particular interest is charcoal, also known as black carbon [13–18]. Charcoal is believed to represent a significant sink in the global carbon cycle [14,19] and some have proposed that it constitutes a significant fraction of aromatics in most humic substances [16,20]. Nevertheless, its identification and quantification have remained difficult and knowledge about its molecular structure is therefore limited. In particular, there are no spectroscopic techniques to distinguish charcoal clearly from other aromatic structures [21], such as lignin or tannins [3–6,22], when they are mixed, for instance in soil organic matter. When activated, charcoal also plays a role in water filtration [15]. Better characterization of the structural changes during the activation process might lead to improved filter performance.

In this paper, we present a new NMR method for distinguishing different types of aromatic carbons based

* Corresponding author. Fax: 1-515-294-0105.
E-mail address: srohr@iastate.edu (K. Schmidt-Rohr).

1090-7807/03/$ - see front matter © 2003 Elsevier Science (USA). All rights reserved.
doi:10.1016/S1090-7807(03)00012-0

on long-range C–H dipolar dephasing, which reflects the distance between the observed carbon site and the nearest proton(s) in the structure. The necessary recoupling of the weak long-range C–H dipolar couplings is achieved by a train of rotation-synchronized 180° pulses, which can be described as a C–H version of the REDOR [23] pulse sequence. Compared to standard dipolar dephasing, also known as "gated decoupling" since decoupling is simply gated off for a certain time, [5,24–31] C–H recoupling increases the dephasing efficiency greatly. This permits the use of long-range dipolar dephasing for effectively suppressing signals of carbon sites with several protons at a two-bond distance, relative to those of carbons more remote from protons. REDOR curves calculated for a simple model of an isolated pair of C–H spins separated by 2, 3, 4, or 5 bonds, Fig. 1, demonstrate that recoupled C–H dipolar dephasing on the millisecond time-scale has the potential of differentiating between unprotonated carbons in different environments. We demonstrate experimentally that recoupled dipolar dephasing can indeed distinguish different sites in a substituted anthraquinone and in 3-methoxy benzamide. From data on nine different unprotonated carbon sites, we construct a calibration curve relating the dephasing rate approximately to the C–H distance, between 2 and ca. 9 Å.

Pulsed recoupling of C–H interactions was recently demonstrated by Vita and Frydman [32], but only to achieve regular dipolar dephasing, i.e. suppress protonated carbon signals, at a relatively high spinning frequency of 12 kHz. Correspondingly, the dephasing time was relatively short (<170 μs). Without a "γ-integral" [33] before detection, that sequence is also prone to sideband artifacts when applied to large, slow-spinning rotors.

In contrast to essentially all previous dipolar dephasing studies, we have performed the experiments presented here with direct polarization (DP) of ^{13}C, rather than ^{1}H–^{13}C crosspolarization (CP), if there was overlap

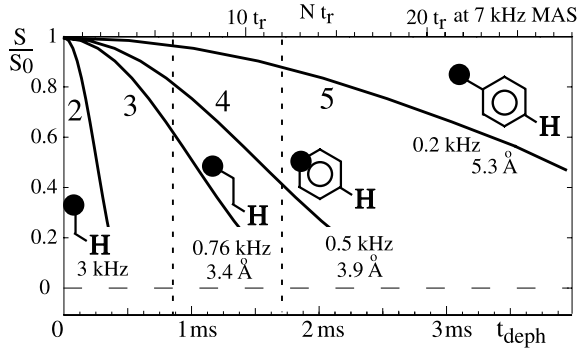

Fig. 1. Model simulations of long-range C–H dipolar dephasing in isolated pairs of ^{13}C and ^{1}H separated by 2, 3, 4, or 5 bonds, under the influence of REDOR C–H dipolar recoupling. Only the initial portions of the curves are shown. C–H internuclear distances and C–H dipolar coupling constant are indicated for the curves.

of protonated- and unprotonated-carbon signals. Being based on C–H dipolar couplings, CP enhances the signals of carbons near protons more than those far away; in extreme cases, carbons very distant from protons are unobservable in CP spectra. Therefore, CP does not provide strong signals of the carbons that are of specific interest in long-range dephasing experiments. We show that a 0.9-ms recoupled dipolar dephasing period in a DP ^{13}C NMR experiment at 7-kHz MAS can clearly discriminate between lignin, charcoal, and carbonate in complex organic matter.

2. Experimental

2.1. Samples

Several model samples were purchased from Sigma–Aldrich–Fluka for the experiments: 3-methoxy benzamide, 1,8-dihydroxy-3-methylanthraquinone, and lignin apparently derived from softwood. A sample of wood charcoal, provided by Prof. Michael Hayes, Ireland, has an elemental composition of 11.1% C, 0.7% H, 1.6% N, 0.05% S, and 1.9% inorganic C (corresponding to 15% of all C; the $CaCO_3$ consists of nearly equal amounts of calcite and dolomite). The carbonate percentage in this sample was determined by the gasometric method [46]. In brief, 1 g of charcoal sieved through a 100-mesh screen was placed into a decomposition flask connected to the Chittick apparatus. Twenty mL 6 M HCl was added into the decomposition flask and allowed to react with carbonate in the charcoal. After the reaction, the volume of CO_2 was recorded and used to calculate the amount of carbonate in charcoal. The standard peat humic acid (HA) and Leonardite HA samples were bought from the International Humic Substances Society (IHSS).

2.2. NMR parameters

Experiments were performed in a Bruker DSX400 spectrometer at 100 MHz for ^{13}C, using a 7-mm magic angle spinning double-resonance probehead. The spinning speed was 7 kHz. Either DP or CP was used. No special tune-up of the spectrometer, other than optimization of pulse lengths, was performed for the experiments. In all the experiments, four-pulse total suppression of sidebands (TOSS) [47] was employed before detection. During detection, TPPM decoupling was applied. The recoupled dipolar dephasing scheme was combined with an incrementation of the z-period preceding TOSS in four steps of $t_r/4$, which provides the "γ-integral"(or "γ-averaging") that suppresses sidebands up to the fourth order [33]. Without this scheme, the signal modulation by partial dephasing resulted in detectable sidebands even after TOSS.

The ^{1}H 90° pulse-length was 4.25 μs and the contact time 2 ms for CP experiments. The ^{13}C 90° and 180°-pulse lengths were 4 and 8.1 μs, respectively. The numbers of scans ranged from 16 to 2048, and recycle delays from 1.3 to 100 s, depending on specific samples and experiments. Before the DP experiments, CP/T_1-TOSS (''Torchia'') experiments [38] were run to find the shortest recycle delay within which all ^{13}C are relaxed to >90% [39]. The dipolar dephasing times varied between 40 μs and 2.6 ms.

3. Results and discussion

3.1. Failure of long-time standard dipolar dephasing

Standard dipolar dephasing destroys the magnetization of protonated carbons by gating the proton decoupling off for ca. 40 μs [21,24,34]. The chemical-shift evolution during this time is refocused into a Hahn echo at 2 t_r, where t_r is the rotation period. This approach achieves selection of unprotonated-carbon signals, at a level of >90% efficiency, and partial selection of methyl-group signals, at ca. 55% efficiency. As an example, the 7-kHz CP/MAS spectrum of 3-methoxy benzamide, Fig. 2a, is shown in Fig. 2b and compared with a spectrum after 40-μs dipolar dephasing, Fig. 2c. The signals of protonated aromatic carbons disappear, while those of the two unprotonated aromatic carbons and the C=O site remain.

To distinguish unprotonated carbon sites at various distances from the nearest proton, especially in the case of fused rings as in charcoal, longer dephasing times are required. However, simply increasing the period during which decoupling is gated off increases the dephasing efficiency only very slowly. Fig. 2d demonstrates that even at a still moderate spinning speed of $\nu_r = 7$ kHz, switching the decoupling off during the long period of 2.25 $t_r = 320$ μs needed for TOSS before detection actually regenerates a significant part of the protonated-carbon signal. The reason is that at the end of each completed rotation period, magic-angle spinning has refocused the C–H dipolar coupling at least partially; this effect is also referred to as a rotational echo and has been observed in various attempts to extend standard dipolar dephasing to long times [21,26,35]. For further discussions of long-time standard dipolar dephasing in the literature, see below.

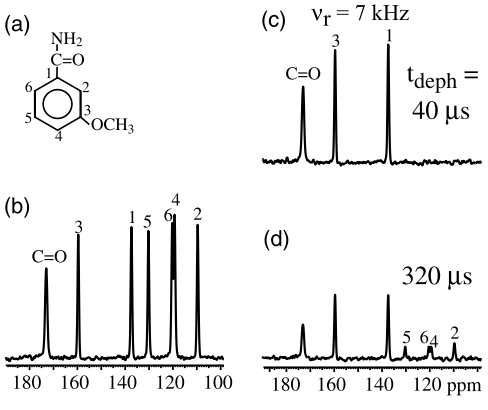

Fig. 2. Demonstration of the failure of standard dipolar dephasing at long dephasing times for 3-methoxy benzamide, at 7 kHz MAS. (a) Structure of 3-methoxy benzamide with carbon numbering. (b) Full CP/TOSS spectrum for reference. (c) CP/TOSS with regular 40-μs dephasing of protonated-carbon signals. (d) Gating decoupling off throughout TOSS, for 320 μs, is seen to fail to remove residual protonated-carbon signal. This shows the failure of standard dipolar dephasing at long dephasing times. A CP contact time of 1 ms was used in these experiments. Measuring time per spectrum: 6.4 min (64 scans).

3.2. Recoupled long-distance dipolar dephasing

The refocusing of anisotropic interactions such as C–H dipolar couplings by MAS can be prevented by rotation-synchronized radio-frequency pulses. Such recoupling of heteronuclear dipolar interactions is achieved most commonly by a train of 180° pulses every half rotation period [23]. A simple example is shown in Fig. 3a. One 180° pulse is applied to ^{13}C in the center of the filter period, in order to refocus the ^{13}C isotropic chemical shift. All the other 180° pulses are applied to ^{1}H. This represents a REDOR [23] pulse sequence for the C–H spin system. Of course, the presence of proton–proton homonuclear as well as multispin ^{1}H–^{13}C heteronuclear couplings prevents the oscillatory behavior characteristic of spin-pair REDOR dephasing curves [23]. Nevertheless, the time constant of the dephasing will reflect the strength of the C–H couplings experienced by the ^{13}C site under consideration. The carbon site is identified by the isotropic chemical shift in the detected spectrum. Finally, the ''γ-integral'' [33],

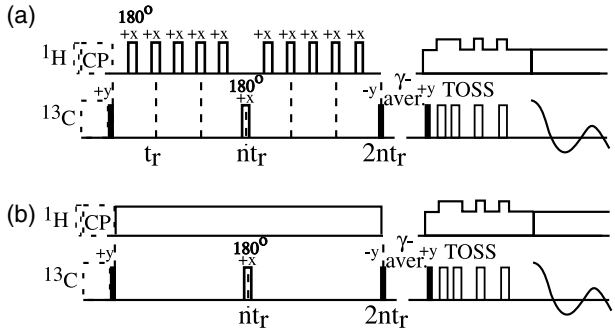

Fig. 3. (a) Pulse sequence for long-range C–H dipolar dephasing. (b) Corresponding sequence to measure T_2 decay, in which no recoupling ^{1}H 180° pulses are used. ^{13}C signal can be generated by CP from protons, as indicated by dashed lines. Preferably, single-pulse excitation of ^{13}C magnetization after a long recycle delay (DP) is used to excite carbons far from protons similarly as protonated carbons. Filled rectangles indicate 90° pulses, while the shortest unfilled rectangles represent 180° pulses.

implemented as a z-filter that is incremented in four steps of $t_r/4$, is important to avoid phase distortions in a regular MAS spectrum, or reintroduction of sidebands into TOSS spectra [36].

The presence of proton homonuclear couplings does not interfere significantly with the C–H dephasing. The main purpose of the 180° pulses is to prevent refocusing of the C–H spin pair interaction by MAS at full rotation periods. If strong homonuclear couplings are present, they achieve a similar dephasing as the 180° pulses, since they dephase the heteronuclear coherences $S_{x/y}I_z$ that are required for the MAS refocusing.

Regular transverse (T_2) relaxation of ^{13}C magnetization that occurs even in the presence of heteronuclear decoupling, e.g. due to interactions of ^{13}C spins with the unpaired electrons of paramagnetic centers, will lead to a signal decay after long dephasing times. The factors to correct for this decay can be determined by recording the signal decay using a simple reference sequence with a Hahn spin echo, as shown in Fig. 3b, where the ^1H 180° pulses are replaced by continuous-wave heteronuclear decoupling. For all aromatic carbon sites studied here, this correction was small compared to the recoupled dephasing.

3.3. Applications to aromatic model compounds

In order to demonstrate differential long-range dipolar dephasing, spectra of a model compound with three substituted fused planar rings, 1,8-dihydoxy-3-methylanthraquinone (Fig. 4a), have been recorded for different dephasing times, see Fig. 4. CP was used for signal generation; the CP/TOSS spectrum, Fig. 4c, shows that all ^{13}C signal were similarly enhanced by CP. Standard dipolar dephasing with a 40-ms gated-decoupling dephasing time, Fig. 4c, destroys the magnetization of protonated aromatic carbons, i.e. carbons 2, 4, 5, 6, and 7. In the spectrum of Fig. 4d obtained after a recoupled dipolar dephasing time of 570 μs, differential long-range C–H dipolar dephasing of the unprotonated carbons is seen clearly. The least dephasing (intensity of 0.28 relative to the full spectrum in Fig. 4d) occurs for carbons 11 and 13, whose nearest proton is three bonds away (C–C–X–H). Carbon 10 and carbons 12 and 14 also dephase relatively slowly, since carbons 12 and 14 have only one proton at a two-bond distance (C–C–H) while carbon 10 has two protons three bonds away (C–C–C–H). Carbons 1, 8 and 3 dephase most (five to eight times more than carbons 13/11) because carbons 1 and 8 both have two protons at a two-bond distance (C–C–H and C–O–H) while carbon 3 has five protons two bonds away (C–C–H). Interestingly, carbon 9, although its nearest protons are four bonds away, still dephases relatively fast. This indicates that the two C–OH protons are at a short through-space distance from carbon 9, as indicated in the structure of Fig. 4a.

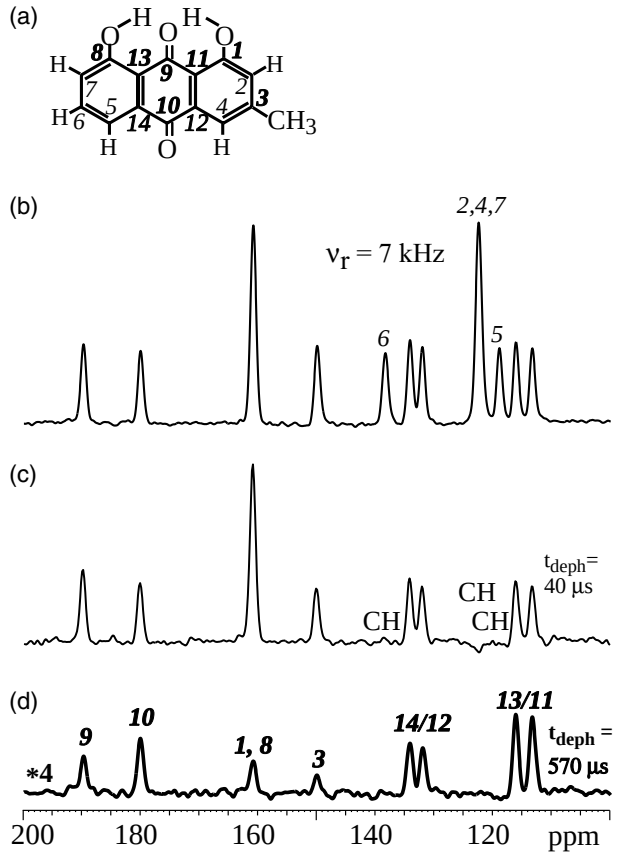

Fig. 4. Differential long-range dipolar dephasing of unprotonated carbons in 1,8-dihydoxy-3-methylanthraquinone, at 7 kHz MAS. (a) Molecular structure and carbon numbering. (b) Full ^{13}C CP/TOSS as reference. (c) CP/TOSS with standard dipolar dephasing of $t_{deph} = 40$ μs. (d) CP/TOSS with recoupled long-range dipolar dephasing of $t_{deph} = 570$ μs, scaled up by a factor of four. The CP contact time was 2 ms. Measuring time for (b) and (c): 27 min (32 scans) and that for (d) 3.6 h (256 scans). Recycle delays were 50 s.

Fig. 5a shows a plot of residual signals, as a function of dephasing time, for the various unprotonated sites in 1,8-dihydoxy-3-methylanthraquinone and in 3-methoxy benzamide. The differential dephasing of the different sites in the former compound has already been discussed. The three unprotonated carbons in 3-methoxy benzamide, see structure in Fig. 2a, all have two protons at a two-bond distance (two C–C–H or two C–N–H) and correspondingly dephase fast (open hexagons, diamonds, and circles). The straight lines obtained for most sites in the semi-logarithmic plot of Fig. 5a indicate exponential dephasing behavior.

In summary, the application of the new technique to two aromatic model compounds has demonstrated that the dephasing rate of unprotonated carbons reflects both the distance from and the number of the nearest protons. In particular, this allows us to differentiate unprotonated carbons with two or more protons at a two-bond distance from carbons that are more distant from their nearest protons.

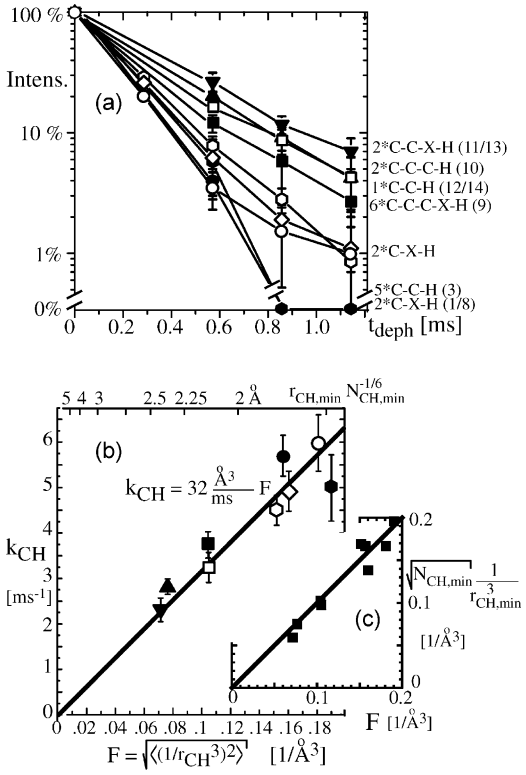

Fig. 5. Long-range dipolar dephasing for 3-methoxy benzamide and 1,8-dihydoxy-3-methylanthraquinone. (a) Dependence of spectral intensities on the dephasing time t_{deph}, in a semi-logarithmic plot. Open symbols are used for carbons with two or more protons at a two-bond distance. The following symbols were used for data from 1,8-dihydoxy-3-methylanthraquinone: inverted filled triangles—average of carbons 11 and 13; filled triangles—carbon 10; open squares—carbons 12 and 14; filled squares—carbon 9; filled hexagons—carbon 3; filled circles—carbons 1 and 8. Symbols for data from 3-methoxy benzamide: open hexagons—unprotonated aromatic carbons, at 137 ppm; open diamonds—aromatic C–O; open circles—C=O. The data were acquired using CP with a contact time of 2 ms. The recycle delays for 3-methoxy benzamide and 1,8-dihydoxy-3-methylanthraquinone were 5 and 50 s, respectively. Total measuring time: 3-methoxy benzamide, 2.5 h; 1,8-dihydoxy-3-methylanthraquinone, 13 h. $\nu_r = 7$ kHz. (b) Plot of initial dephasing rates k_{CH} vs. intramolecular dipolar dephasing factors F. At the top of the figure, effective distances $r_{CH,min}N_{CH,min}^{-1/6}$ are indicated. (c) Correlation of $F_{CH,min} = N_{CH,min}^{1/2} r_{CH,min}^{-3}$, calculated from the minimum C–H distances only, and the full dipolar dephasing factor F. The thick line is the diagonal of the plot.

3.4. Quantitative evaluation

As a more quantitative measure of the total CH dipolar couplings of a given carbon, we have calculated an intramolecular dipolar "distance factor"

$$F = \sqrt{\left\langle \left(\frac{1}{r_{CH}^3} \right)^2 \right\rangle} = \sqrt{\sum_n \frac{1}{r_{CH,n}^6}} \tag{1}$$

with the distance $r_{CH,n}$ between the carbon of interest and the nth proton. For simplicity, the sum is restricted to the protons within the same molecule as the carbon, and at less than 5-Å distance. The value of F in Eq. (1) is proportional to the square-root of the second moment of the C–H dipolar coupling [37], i.e. to the root-mean-square width of the C–H dipolar spectrum. For the CH_3 protons, motional averaging of C–H couplings has been taken into account by means of appropriate prefactors in front of the methyl-proton $1/r_{CH}^6$-terms in the sum of Eq. (1).

Due to its proportionality to the average overall dipolar coupling, we expect F to be proportional to the initial rate k_{CH} (i.e. the inverse of the exponential-decay constant τ_{CH})

$$k_{CH} = 1/\tau_{CH} = \frac{-\ln[I(0.57\,\text{ms})/I(0)]}{0.57\,\text{ms}} \tag{2}$$

of the C–H dipolar dephasing curves $I(t) = I(0)\exp(-t/\tau_{CH})$ shown in Fig. 5a. Fig. 5b confirms this correlation of k_{CH} and F satisfactorily. A best-fit line through the origin is also shown, which will permit estimates of F from k_{CH} in complex organic matter. Its slope of 32 ± 2 kHz Å^3 closely matches the C–H dipolar coupling constant (30 kHz/[r_{CH}/Å]^3).

The correlation between k_{CH} and the intramolecular distance factor F can be used as a new tool of systematic resonance assignment in molecules with heavily substituted or fused aromatic ring systems. One calculates F for each unprotonated site in a proposed model structure, and uses the calibration curve, or simply the relative values of F, to predict a sequence of k_{CH} values. Matching the predicted and measured k_{CH} results will provide tentative assignments of many aromatic sites. Note that even for the three unprotonated carbons of 3-methoxy benzamide, which all have the nearest proton at a two-bond distance, this assignment strategy would have provided the correct peak identification.

3.5. Estimating C–H distances

In the sum of Eq. (1), the contributions from the smallest distances $r_{CH,min}$ dominate. This is confirmed by Fig. 5c, which shows a plot of the full dipolar distance factor F against its simple approximation,

$$F_{CH,min} = \sqrt{N_{CH,min}}\,\frac{1}{r_{CH,min}^3}, \tag{3}$$

where we define $N_{CH,min}$ as the number of protons within 1.25 $r_{CH,min}$ from the carbon. Through the relationship between k_{CH}, F, and $\sqrt{N_{CH,min}}(1/r_{CH,min}^3)$, the dephasing curves can yield estimates of the distance $r_{CH,min}N_{CH,min}^{-1/6} = F_{CH,min}^{-1/3} \approx F^{-1/3}$. This distance variable is indicated at the top of Fig. 5b and will be used below for estimating $r_{CH,min} \approx F^{-1/3}N_{CH,min}^{+1/6}$ in various samples of natural organic matter. Since $N_{CH,min}^{+1/6}$ varies weakly with $N_{CH,min}$ and is close to unity, $r_{CH,min}$ can be estimated with limited error. For instance, the large uncertainty in $N_{CH,min} = 6 \pm 4$ results only in a relatively limited uncertainty in $N_{CH,min}^{+1/6} = 1.29 \pm 0.17$.

3.6. Discussion of intermolecular contributions

Our simple analysis in terms of only intramolecular C–H distances is seen to produce consistent results. For the unprotonated aromatic sites of interest here, intermolecular contributions are usually small, for the following reasons. The closest approach of planes of stacked aromatic rings, as in graphite, is 3.4 Å, and the closest distance to a proton in a neighboring plane is typically larger, since the probability of a proton being located exactly above the unprotonated carbon of interest is small. In terms of the lateral approach of aromatic molecules, it is important to consider that for the unprotonated aromatic carbons that we are studying, bulky substituents such as CH_n, OH, or OCH_n groups are present on all sides and block the close approach of protonated groups of neighboring molecules. As a result, the intermolecular C–H distances significantly exceed the smallest intramolecular C–H distances for most sites in our model compounds.

Hydroxyl substituents are an exception, in that they can attract intermolecular hydrogen-bonding partners to close distances. In 1,8-dihydoxy-3-methylanthraquinone, the C–OH resonances indeed dephase faster than predicted based on the intramolecular calibration curve (filled circle in Fig. 5b), although the intramolecular dephasing by the OH proton is still a major factor. It should be noted that these phenolic sites are not relevant for the potential charcoal resonances near 130 ppm, since the chemical shift excludes OH groups from being directly bonded to 130-ppm sites (phenols resonate more downfield, near 150 ppm) or bonded to neighboring carbons (aromatic C=C–O sites resonate more upfield, near 110 ppm).

3.7. Charcoal vs. lignin

Fig. 6 shows series of DP/TOSS ^{13}C NMR spectra of wood char (Fig. 6a) and softwood lignin (Fig. 6b) with increasing recoupled dephasing times. CP/T_1/TOSS "Torchia" experiments [38] were used for efficient tests that the recycle delays yield more than 90% of the fully relaxed intensities [39]. Compared with the lignin spectra, those of wood char are simple, exhibiting only two bands. The band centered at around 125 ppm is due to charcoal aromatics, while the sharp peak at around 169 ppm arises from the CO_3^{2-} carbons in this sample. In lignin, substitution of the aromatic rings by several oxygens, see Fig. 6c, results in a variety of carbon chemical shifts. Fig. 6 shows that at a recoupled dipolar dephasing time of 0.86 ms, almost all the signals of softwood lignin have been dephased, while more than half of the charcoal aromatic signals remain. In fact, even after a dipolar dephasing time of 2.6 ms, the aromatic signal of wood charcoal is still significant (25% after slight T_2 correction obtained from the sequence of Fig. 3b). This

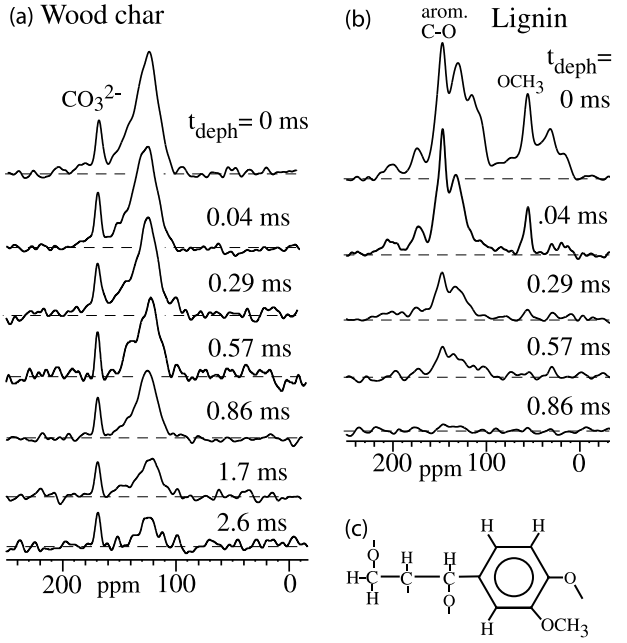

Fig. 6. Series of DP/TOSS spectra after recoupled dipolar dephasing of the indicated durations t_{deph}. (a) Wood char with 20-s recycle delay. Differences in the noise levels result from different numbers of scans (taken into account in the plots). (b) Lignin with 60-s recycle delay. (c) Structure of a typical softwood-lignin unit. Total measuring times of 27 h for (a) and 21 h for (b), at $\nu_r = 7$ kHz.

shows that many aromatic carbons in wood charcoal are farther away from protons than those of softwood lignin, consistent with the more condensed character expected of wood-char aromatics.

3.8. Carbonate carbon

In addition to the main aromatic band, the spectra of Fig. 6a also show a sharp, very slowly dephasing C=O signal around 169 ppm. Chemical-shift anisotropy measurements have confirmed that this is not a mobile impurity but a rigid solid. It is so far from any protons that it is not observable in CP experiments. The signal must be due to inorganic carbonate in the sample, which was shown by gasometric analysis to account for ca. 15% of all carbon in the sample. The isotropic chemical shift of 169 ppm confirms this assignment [40].

3.9. Application to humic acids

Based on the slow dephasing of charcoal signals relative to partially protonated single-ring aromatics, the new method can be used to identify whether charcoal-like fused aromatic rings are present in natural organic matter. Fig. 7 presents an application of this technique to IHSS (International Humic Substances Society) standard peat HA and Leonardite HA. The resulting dephasing curves of the aromatic carbons not bonded to oxygen (signal between 107 and142 ppm) are presented

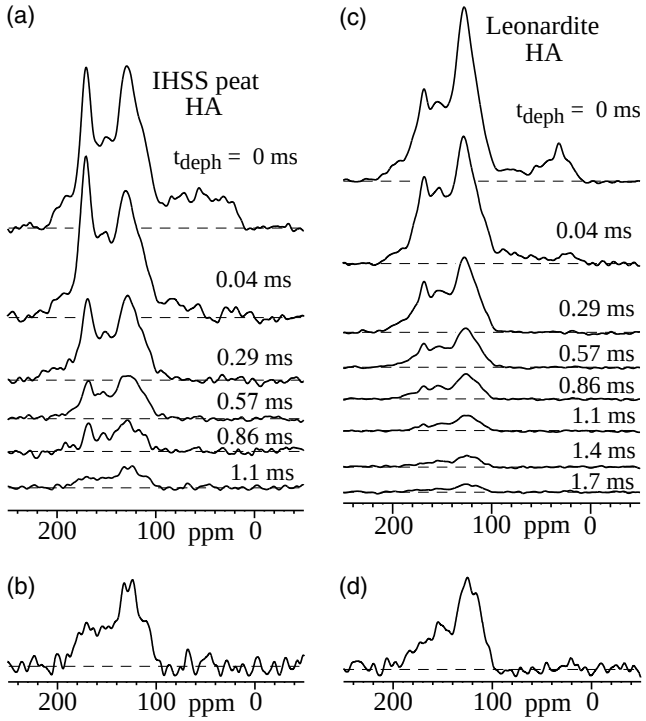

Fig. 7. Series of DP/TOSS spectra after recoupled dipolar dephasing of the indicated durations t_{deph}. (a) IHSS peat HA with 25-s recycled delay. (b) Enlarged plot of the spectrum in (a) with the longest dephasing time (1.1 ms). (c) IHSS Leonardite (oxidized brown coal) HA with 10-s recycled delay. Total measuring times of 12 h for (a) and 34 h for (c), at 7-kHz MAS. (d) Enlarged plot of the sum of the two spectra in (c) with the longest dephasing times (1.4 and 1.7 ms).

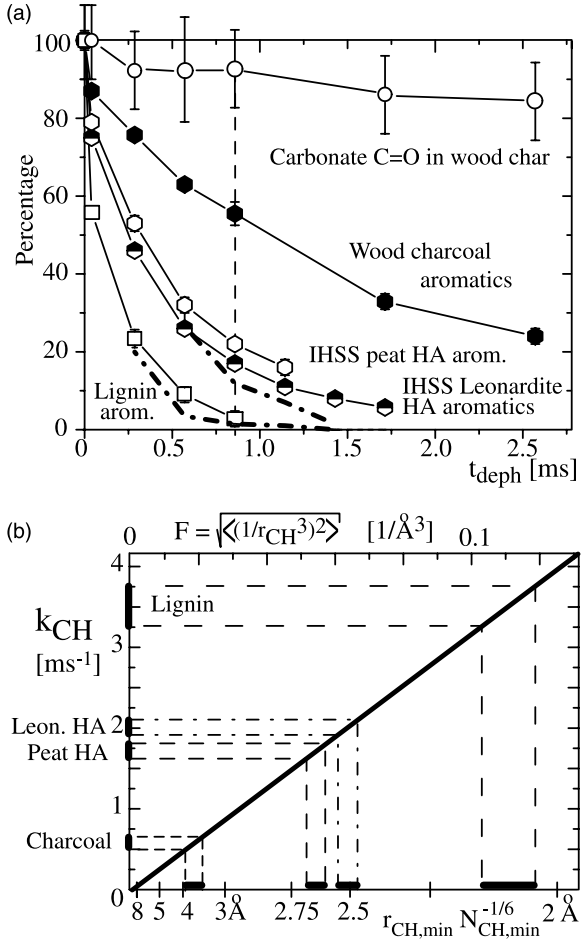

Fig. 8. (a) Long-range dipolar dephasing curves for wood charcoal, inorganic carbonate in wood char, IHSS peat HA, IHSS Leonardite (oxidized brown coal) HA, and lignin, obtained from the DP/TOSS spectra shown in Figs. 6 and 7. The aromatic signals were integrated between 107 and 142 ppm. Filled hexagons: wood-char aromatics; open hexagons: IHSS peat HA aromatics; half-filled hexagons: IHSS Leonardite HA aromatics; open squares: lignin aromatics. Open circles: inorganic carbonate in wood char. The data points have been corrected slightly for regular T_2 relaxation, measured with the sequence of Fig. 3b. In order to facilitate comparison with the data shown in Fig. 5a, the top and bottom curves from that figure have been included here as dash-dotted lines. (b) Calibration curve of Fig. 5b (straight line through the origin), with the dephasing rates from (a) and corresponding values of $r_{CH,min}N_{CH,min}^{-1/6}$ indicated. From the distance values on the x-axis, $r_{CH,min}$ is obtained by multiplication with $N_{CH,min}^{+1/6}$.

in Fig. 8a and compared with those of wood charcoal and softwood lignin. The top and bottom curves from the model compounds in Fig. 5a are also shown for comparison.

The relatively slow decay of the peaks near 127 ppm in the HA samples, see Fig. 7, shows that recoupled long-range dipolar dephasing indeed achieves some selection of aromatic carbons not bonded to oxygens, relative to aromatic C–O carbons. At the dipolar dephasing time of 0.86 ms, 22% of IHSS peat HA and 17% of Leonardite HA non-polar aromatic signals are left, in contrast to 55% aromatic signal of wood char and essentially no signal of lignin. At long times, the dephasing curves for the humic acids are clearly non-exponential, while the dephasing in the homogeneous model compounds was remarkably exponential in nature, see Fig. 5. For Leonardite HA, using the non-protonated aromatic signal of 75% as the full reference intensity, the non-protonated aromatic signal has dephased to 26%/0.75 = 35% after 0.58 ms. Assuming exponential dephasing, the signal at $t_{deph} = 1.7$ ms would be $(0.35)^3 = 4.3\%$, while the observed intensity is larger, at 5.7%/0.75 = 7.6% of the non-protonated aromatic signal. We attribute this significant slow-down of the signal decrease at long times to the presence of a slowly-dephasing fraction, whose dephasing appears to resemble that of the charcoal sample. We can estimate the amount of this fraction in the humic acid as follows.

At the dipolar dephasing time of 1.7 ms, ca. 5% of charcoal-like aromatic signals remain for the Leonardite HA, while the wood-char aromatic signals have been dephased by a factor of 1/3. Thus, the full signal of these charcoal-like components in the humic acid would correspond to ca. $3 \times 5\% = 15\%$ of fused aromatic rings in this signal. Figs. 7b and d show enlarged plots of the HA spectra at the longest dephasing times. They are

significantly different from the unfiltered spectra of the HAs at the top of Figs. 7a and c, showing characteristics of oxidized charcoal with increased 130-ppm aromatic and reduced C=O signals.

The experiments show that the fraction of large charcoal-like clusters of polycondensated aromatic rings is relatively low in both HAs. For Leonardite HA, ca. 5% of all carbons are part of such larger ring systems. This number is obtained from the 15% value derived above, given that the signal between 107 and 142 ppm corresponds to approximately 1/3 of all carbons in Leonardite HA. The majority of the aromatics in the HAs are found to consist of two or three fused rings, or densely substituted single aromatic rings. They are less protonated than the individual rings in lignin, which contain at least two protonated carbons. The slightly slower decay of the IHSS peat HA signals indicates that these aromatics are somewhat more condensed than those of IHSS Leonardite HA. This may be surprising, since Leonardite HA has been extracted from an air-oxidized brown coal, which might be expected to contain larger fused ring systems than the subtropical peat humic acid.

At a dephasing time around 0.9 ms, marked by the dashed vertical line in Fig. 8a, we can dephase softwood-lignin signals to less than 3%, while retaining charcoal signal at a 55% level. This condition combines good sensitivity for fused rings with clean suppression of signals from only partially substituted individual aromatic rings.

3.10. Estimated C–H distances in natural organic matter

Based on the calibration of dephasing rates k_{CH} vs. C–H distances shown in Fig. 5b, the data of Fig. 8a can be used to obtain rough estimates of the closest C–H distances of the unprotonated aromatic carbons in the four samples of natural organic matter. Fig. 8b shows the calibration curve, with the dephasing rates extracted from Fig. 8a indicated on the y-axis. Only the dephasing of the unprotonated carbons was considered, by calculating

$$k_{CH} = -\ln[I(0.57\,\text{ms})/I(0.04\,\text{ms})]/\{0.57\,\text{ms} - 0.04\,\text{ms}\}. \quad (4)$$

Fig. 8b shows that the corresponding distances $r_{CH\,min}N_{CH,min}^{-1/6}$, according to the calibration curve, are 2.1 Å for lignin, 2.5 Å for IHSS Leonardite HA, 2.6 Å for IHSS peat HA, and 3.7 Å for wood charcoal. The carbonate data were not evaluated, since the decay observed is probably mostly due to a small background of charcoal C=O groups (see Fig. 6a). We estimate that $N_{CH,min} = 6 \pm 4$, with generous uncertainties. This yields $r_{CH,min} = 2.7 \pm 0.4$ Å for softwood lignin, $r_{CH,min} = 3.2 \pm 0.5$ Å for the Leonardite HA, 3.4 ± 0.5 Å for the peat HA, and $r_{CH,min} = 4.8 \pm 1$ Å for wood-char aromatics. Given the distribution of C–H distances of unprotonated aromatics expected in natural organic matter, these distances should only be taken as estimates of typical values. The C–H distance estimate for charcoal may seem surprisingly short, but comparison of the dephasing curves in Fig. 8a and the model calculations of Fig. 1 confirm that the observed dephasing corresponds to C–H distances of less than 10 Å. A more detailed discussion of the size of fused aromatic ring systems in charcoal and soil organic matter obtained from these and other measurements will be published elsewhere [41].

3.11. Direct polarization vs. crosspolarization

In the long-range dephasing spectra of natural organic matter shown above, we used DP of ^{13}C rather than CP. This is important for obtaining spectra of natural organic matter in which the charcoal fraction is represented significantly. The carbons to be selected by the long-range dipolar dephasing are necessarily far removed from the nearest protons. Use of CP would reduce their relative intensity and thus make them less prominent, since CP efficiencies decrease with the C–H coupling strength. This effect has been neglected in essentially all previous attempts of long-range dipolar dephasing (which in addition also used the less efficient unrecoupled gated decoupling) [5,21,26,27,29–31]. As a result, the signals for charcoal could never be selected cleanly [21].

Fig. 9 compares recoupled dipolar dephasing of CP vs. DP signals on charcoal and lignin. In order to reduce the suppression of unprotonated-carbon signals in the CP spectrum, a relatively long contact time of 2 ms was employed; much longer CP times are not practical due to the short $T_{1\rho}$ relaxation in many samples of natural organic matter. The predicted signal distortion by CP is

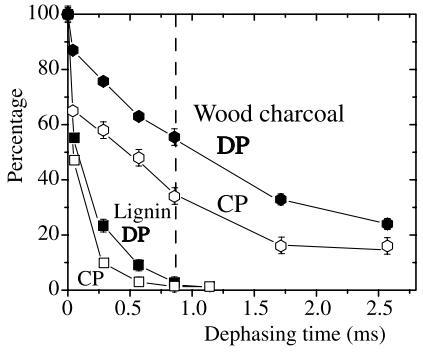

Fig. 9. Comparison of long-range dipolar dephasing after CP (contact time of 2 ms) and DP, for charcoal (top curves) and lignin (bottom curves). DP: Filled symbols; CP: open symbols. Charcoal aromatic signals are indicated by filled (DP) and open (CP) hexagons, lignin aromatic signals between 107 and 142 ppm by filled (DP) and open (CP) squares. The DP data are the same as in Fig. 8. Measuring times for charcoal and lignin CP data: 8 and 1.5 h, respectively.

seen to be strong. For instance, in charcoal after 0.86 ms of dephasing, the normalized CP signal is reduced by a factor of 1.6 relative to the normalized DP signal. The main reason for this difference is overlap of unprotonated- and protonated-carbon signals; if the latter are enhanced in the CP spectrum, they raise the reference signal level $I_{CP}(t_{deph} = 0)$. Unprotonated carbons two bonds from protons are also expected to be enhanced in the CP spectrum. A CP-induced charcoal signal reduction as seen in Fig. 9 would severely impact the selection of a charcoal fraction out of a background of other aromatics. Fig. 9 also demonstrates that even in softwood lignin, where most unprotonated carbons have two protons at a two-bond distance, the signal after DP dephases more slowly than that after long CP. Again, overlap with protonated carbons explains much of the difference between CP and DP.

3.12. Comparison with standard long-time recoupling

For many years, soil scientists have pursued similar goals as were achieved here, but using standard dipolar dephasing without recoupling after CP [5,21,26,27,29–31]. This traditional approach has two major shortcomings: (i) The dephasing is an inefficient, spinning-speed dependent second-order effect and (ii) CP suppresses the unprotonated signals of interest. As a result, charcoal selection could not be achieved [21].

Without H–H couplings, standard dipolar dephasing is periodic with t_r, since MAS refocuses the C–H coupling at full rotation periods; in other words, dephasing would not become stronger with time beyond the dephasing at $t_r/2$. Being due only to second-order interference between non-commuting C–H and H–H dipolar interactions, long-time standard dipolar dephasing is more difficult to interpret, since it depends significantly on the homonuclear interactions of the protons surrounding the carbon of interest. In addition, the second-order nature makes this unrecoupled dephasing inefficient. For instance, the aromatic carbons in lignin (130 ppm) are dephased only to 18–36% at 750-μs unrecoupled dephasing time, see Fig. 8 of [21]; the same dephasing can be achieved within 250 μs with our recoupled dephasing technique. Note that in early attempts of long-range dipolar dephasing [26], the chemical-shift anisotropy was also recoupled [35], leading to artificial additional dephasing of aromatic signals by a factor of 0.6.

Without recoupling, the standard dephasing at long times depends not only on the C–H dipolar couplings, but also crucially on spinning-speed dependent effective proton–proton interactions [42,43]. At higher spinning frequencies, the H–H couplings are progressively averaged and dephasing will slow down. Already at $\nu_r = 5$ kHz, the dephasing efficiency is low [21]. Why are high spinning speeds needed? In modern high-field spectrometers, aromatic carbons cannot be detected with good sensitivity at low spinning frequencies, since too much intensity is lost into the sidebands arising from the field-proportional chemical-shift anisotropies. Why not work at low fields? For obtaining undistorted spectra of charcoal, DP is necessary, since CP of carbons in the centers of fused ring systems is too inefficient. At low fields, the sensitivity is often too low for quantitative DP spectroscopy. Thus, for NMR of charcoal, high-field measurements at sufficiently fast spinning rates are recommended. These combine well with the simple recoupled dipolar dephasing presented here.

The low efficiency of unrecoupled dephasing makes long dephasing times necessary, which in turn reduces the sensitivity. Signal loss due to other, unrelated T_2 relaxation mechanisms such as paramagnetic dephasing can exceed 15% at 1.7 ms of dephasing in the case of wood char. At the three-times longer time needed for comparable standard dipolar dephasing, the "regular" T_2 decay, e.g. due to paramagnetics, would destroy more than 40% of the signal. In the constant-time experiment as described in [21], the sensitivity in all experiments is reduced, which may excessively increase the measuring time needed for DP spectroscopy.

As a result of these various short-comings, standard dipolar dephasing data as shown, for instance, in [21] do not achieve any selection of charcoal signal; in fact, charcoal signals have been dephased more than some of the lignin peaks, see Fig. 8 of [21]. To a large part, this is due to the use of CP, which greatly underrepresents the unprotonated carbons in charcoal. In studies that, like [21], would like to claim "quantitative" ^{13}C NMR analysis of charcoal-containing samples, DP is indispensable [44]. The signal distortions by CP have also afflicted the numerous studies that have used medium-range dipolar dephasing to study aromatics in coals and soil organic matter [5,27,29–31,45]. These investigations have only been able to separate protonated aromatics from unprotonated aromatics. Our work is the first to cleanly separate signals of unprotonated aromatics at different distances from protons.

Once programmed, the pulse sequence introduced here is not more difficult to apply than the regular dipolar dephasing. The only parameters to be set are the power levels to achieve the correct 90° and 180° pulse lengths of ^1H and ^{13}C, which is part of any routine set-up of CP/TOSS NMR.

4. Conclusions

A convenient new NMR technique for distinguishing various aromatics based on long-range C–H dipolar dephasing has been demonstrated on both model compounds and complex natural organic matter. It

recouples the C–H dipolar coupling by a simple train of ^{1}H 180° pulses. Calibration on model compounds permits conversion of the dephasing rates into estimates of typical nearest C–H distances of unprotonated aromatics, between 2 and 9 Å. After a dephasing time of ca. 0.9 ms, all lignin signals have been suppressed, while those of interior carbons in condensed aromatics are significantly retained. This technique is particularly useful for identifying charcoal in natural organic matter. We have shown that it should be combined with direct ^{13}C polarization, rather than CP, in order to avoid up to 1.6-fold suppression of the unprotonated sites of interest, which have low CP efficiencies.

Acknowledgments

The authors would like to thank the National Science Foundation (Grant CHE-0138117) for partial financial support. The wood charcoal sample was kindly provided by Prof. Michael Hayes, University of Limerick, Ireland. The assignment of the carbonate peak was suggested to us by Mark Solum, University of Utah.

References

[1] F.J. Stevenson, Humus Chemistry: Genesis, Composition, Reactions, second ed., Wiley, New York, 1994.
[2] V.J. Bartuska, G.E. Maciel, H.I. Bolker, B.I. Fleming, Structural studies of lignin isolation procedures by ^{13}C NMR, Holzforschung 34 (1980) 214–217.
[3] G.E. Maciel, D.J. O'Donnell, J.J.H. Ackerman, B.H. Hawkins, V.J. Bartuska, A ^{13}C NMR study of four lignins in the solid and solution states, Makromol. Chem. 182 (1981) 2297–2304.
[4] J.F. Haw, G.E. Maciel, H.A. Schroeder, Carbon-13 nuclear magnetic resonance spectrometric study of wood and wood pulping with cross polarization and magic-angle spinning, Anal. Chem. 56 (1984) 1323–1329.
[5] P.G. Hatcher, Chemical structural studies of natural lignin by dipolar dephasing solid-state carbon-13 nuclear magnetic resonance, Org. Geochem. 11 (1987) 31–39.
[6] K.R. Morgan, R.H. Newman, Principal values of ^{13}C NMR chemical shift tensors for a collection of substituted benzenes, J. Am. Chem. Soc. 112 (1990) 4–7.
[7] K.B. Anderson, R.E. Winans, R.E. Botto, The nature and fate of natural resins in the geosphere—II. Identification, classification and nomenclature of resinites, Org. Geochem. 18 (1992) 829–841.
[8] R.E. Botto, in: D.M. Grant, R.K. Harris (Eds.), Encyclopedia of Nuclear Magnetic Resonance, vol. 3, Wiley, New York, 1996, pp. 2101–2118.
[9] A.M. Gil, C.P. Neto, Solid-state NMR studies of wood and other lignocellulosic materials, Ann. Rep. NMR Spectrosc. 37 (1999) 75–117.
[10] J.Z. Hu, M.S. Solum, C.M.V. Taylor, R.J. Pugmire, D.M. Grant, Structural determination in carbonaceous solids using advanced solid state NMR techniques, Energy Fuels 15 (2001) 14–22.
[11] J.-D. Mao, B. Xing, K. Schmidt-Rohr, New structural information on a humic acid from two-dimensional ^{1}H-^{13}C correlation solid-state nuclear magnetic resonance, Environ. Sci. Technol. 35 (2001) 1928–1934.
[12] N. Hertkorn, A. Permin, I. Permina, D. Kovalevskii, M. Yudov, V. Petrosyan, A. Kettrup, Comparative analysis of partial structures of a peat humic and fulvic acid using one- and two-dimensional NMR spectroscopy, J. Environ. Qual. 31 (2002) 375–387.
[13] M.W.I. Schmidt, Black carbon in soils and sediments: analysis, distribution, inplications, and current challenges, Global Biogeochem. Cycles 14 (2000) 777–793.
[14] T.A.J. Kuhlbusch, Black carbon and the carbon cycle, Science 280 (1998) 1903–1904.
[15] E.D. Goldberg, Black Carbon in the Environment, Wiley, New York, 1985.
[16] J.O. Skjemstad, P. Clarke, J.A. Taylor, J.M. Oades, S.G. McClure, The chemistry and nature of protected carbon in soil, Aust. J. Soil Res. 34 (1996) 251–271.
[17] B. Glaser, L. Haumaier, G. Guggenberger, W. Zech, Black carbon in soils: the use of benzenecarboxylic acids as specific markers, Org. Geochem. 29 (1998) 811–819.
[18] R.J. Smernik, J.O. Skjemstad, J.M. Oades, Virtual fractionation of charcoal from soil organic matter using solid state ^{13}C NMR spectral editing, Aust. J. Soil Res. 38 (2000) 665–683.
[19] R.J. Scholes, I.R. Noble, Storing carbon on land, Science 294 (2001) 1012–1013.
[20] J.O. Skjemstad, J.A. Taylor, R.J. Smernik, Estimation of charcoal (char) in soils, Commun. Soil Sci. Plant Anal. 30 (1999) 2283–2298.
[21] R.J. Smernik, J.M. Oades, Solid-state ^{13}C-NMR dipolar dephasing experiments for quantifying protonated and non-protonated carbon in soil organic matter and model systems, Eur. J. Soil Sci. 52 (2001) 103–120.
[22] C.M. Preston, J.A. Trofymow, B.G. Sayer, J. Niu, ^{13}C NMR spectroscopy with CP/MAS investigation of the proximate-analysis fractions used to assess litter quality in decomposition studies, Can. J. Bot. 75 (1997) 1601–1613.
[23] T. Gullion, J. Schaefer, Rotational-echo double-resonance NMR, J. Magn. Reson. 81 (1989) 196–200.
[24] S.J. Opella, M.H. Frey, Selection of nonprotonated carbon resonances in solid-state nuclear magnetic resonance, J. Am. Chem. Soc. 101 (1979) 5854–5856.
[25] P.D. Murphy, B.C. Gerstein, V.L. Welnberg, T.F. Yen, Determination of chemical functionality in asphaltenes by high-resolution solid-state carbon-13 nuclear magnetic resonance spectrometry, Anal. Chem. 54 (1982) 522–525.
[26] L.B. Alemany, D.M. Grant, T.D. Alger, R.J. Pugmire, Cross polarization and magic angle sample spinning NMR spectra of model organic compounds. 3. Effect of the ^{13}C–^{1}H dipolar interaction on cross polarization and carbon–proton dephasing, J. Am. Chem. Soc. 105 (1983) 6697–6704.
[27] M.A. Wilson, R.J. Pugmire, D.M. Grant, Nuclear magnetic resonance spectroscopy of soils and related materials. Relaxation of ^{13}C nuclei in cross polarization nuclear magnetic resonance experiments, Org. Geochem. 5 (1983) 121–129.
[28] A.H. Gillam, M.A. Wilson, P.J. Collin, Structural analysis of sea loch sedimentary humic substances by carbon-13/hydrogen-1 dipolar dephasing NMR, Org. Geochem. 11 (1987) 91–101.
[29] M.A. Wilson, B.D. Batts, P.G. Hatcher, Molecular composition and mobility of torbanite precursors: implications for the structure of coal, Energy Fuels 2 (1988) 668–672.
[30] P.G. Hatcher, H.E. Lerch III, A.L. Bates, T.V. Verheyen, Solid-state ^{13}C nuclear magnetic resonance studies of coalified gymnosperm xylem tissue from Australian brown coals, Org. Geochem. 14 (1989) 145–155.
[31] P.G. Hatcher, M. Schnitzer, A.M. Vassallo, M.A. Wilson, The chemical structure of highly aromatic humic acids in three volcanic ash soils as determined by dipolar dephasing NMR studies, Geochim. Cosmochim. Acta 53 (1989) 125–130.
[32] E.D. Vita, L.F. Frydman, Spectral editing in ^{13}C MAS NMR under moderately fast spinning conditions, J. Magn. Reson. 148 (2001) 327–337.

[33] E.R. deAzevedo, W.-G. Hu, T.J. Bonagamba, K. Schmidt-Rohr, Principles of centerband-only detection of exchange in solid state NMR and extentions to four-time CODEX, J. Chem. Phys. 112 (2000) 8988–9001.
[34] P.G. Hatcher, Dipolar-dephasing ^{13}C NMR studies of decomposed wood and coalified xylem tissue: evidence for chemical structural changes associated with defunctionalization of lignin structural units during coalification, Energy Fuels 2 (1988) 48–58.
[35] R.H. Newman, Chemical-shift anisotropies can dominate dephasing in "dipolar dephasing" CP/MAS NMR experiments, J. Magn. Reson. 96 (1992) 370–375.
[36] K. Schmidt-Rohr, H.W. Spiess, Multidimensional Solid-State NMR and Polymers, first ed., Academic Press, London, 1994.
[37] A. Abragam, Principles of Nuclear Magnetism, Oxford University Press, Oxford, 1961.
[38] D.A. Torchia, The measurement of proton-enhanced Carbon-13 T1 values by a method which suppresses artifacts, J. Magn. Reson. 30 (1978) 613–616.
[39] J.-D. Mao, W.-G. Hu, K. Schmidt-Rohr, G. Davies, E.A. Ghabbour, B. Xing, Quantitative characterization of humic substances by solid-state ^{13}C NMR, Soil Sci. Soc. Am. J. 64 (2000) 873–884.
[40] T.M. Duncan, A compilation of chemical shift anisotropies, Farragut, Chicago, 1997.
[41] J.-D. Mao, M.L. Thompson, M.H.B. Hayes, K. Schmidt-Rohr, NMR analysis of aromatic compounds in natural organic matter 1. Charcoal and related structures, to be submitted (2003).
[42] C. Filip, S. Hafner, I. Schnell, D.E. Demco, H.W. Spiess, Solid-state NMR spectra of dipolar-coupled multi-spin systems under fast magic-angle spinning, J. Chem. Phys. 110 (1999) 423–440.
[43] D. Reichert, T.J. Bonagamba, K. Schmidt-Rohr, Slow-down of ^{13}C spin diffusion in organic solids by fast MAS: a CODEX NMR study, J. Magn. Reson. 151 (2001) 129–135.
[44] R.J. Smernik, J.M. Oades, The use of spin counting for determining quantitation in solid-state ^{13}C NMR spectra of natural organic matter 1. Model systems and the effects of paramagnetic impurities, Geoderma 96 (2000) 102–129.
[45] C.E. Snape, D.E. Axelson, R.E. Botto, J.J. Delpuech, P. Tekely, B.C. Gerstein, M. Pruski, G.E. Maciel, M.A. Wilson, Quantitative reliability of aromaticity and related measurements on coals by ^{13}C NMR; a debate, Fuel 68 (1989) 547–560.
[46] A. Dreimanis, Quantitative gasometric determination of calcite and dolomite by using Chittick apparatus, J. Sediment. Petrology 32 (1962) 520–529.
[47] W.T. Dixon, Spinning-sideband-free and spinning-sideband-only NMR spectra of spinning samples, J. Chem. Phys. 77 (1982) 1800–1809.